

NNLO Corrections to the Higgs Production Cross Section.

V. Ravindran,^{a*} J. Smith,^b W.L. van Neerven.^c

^aHarish-Chandra Research Institute, Chhatnag Road, Jhusii, Allahabad, 211019, India.

^bC.N. Yang Institute for Theoretical Physics, State University of New York at Stony Brook, New York 11794-3840, USA

^cInstituut-Lorentz, Universiteit Leiden, PO Box 9506, 2300 RA Leiden, The Netherlands.

We discuss the next-to-next-to-leading order (NNLO) corrections to the total cross section for (pseudo-) scalar Higgs boson production. The computation is carried out in the effective Lagrangian approach which emerges from the standard model by taking the limit $m_t \rightarrow \infty$ where m_t denotes the mass of the top quark.

The Higgs boson (H) has not yet been discovered. Recently a new central value for the top quark mass of $m_t = 178.0$ GeV/c² was reported [1] so that the lower limit on the mass of the Higgs from the LEP experiments is now $m \sim 117$ GeV/c² [2]. The search for the Higgs boson is a high priority item at the Tevatron and at the future LHC.

In this contribution we discuss H production via the gluon-gluon fusion mechanism. In the standard model the H-g-g coupling contains quark loops. Since the H - q - \bar{q} coupling is proportional to the mass of the quark the top-quark loop gives the largest cross section. The calculations simplify if one takes the limit $m_t \rightarrow \infty$ and uses the heavy quark effective theory (HQET) containing a direct Hgg coupling. Studies show that this is also an excellent approximation. The Lagrangian density is

$$\mathcal{L}_{eff}^H = G_H \Phi^H(x) O(x), \quad (1)$$

with

$$O(x) = -\frac{1}{4} G_{\mu\nu}^a(x) G^{a,\mu\nu}(x), \quad (2)$$

whereas pseudo-scalar Higgs (A) production is obtained from

$$\mathcal{L}_{eff}^A = \Phi^A(x) \left[G_A O_1(x) + \tilde{G}_A O_2(x) \right] \quad (3)$$

*Deutsches Elektronen-Synchrotron DESY, Platanenallee 6, 15738 Zeuthen.

with

$$O_1(x) = -\frac{1}{8} \epsilon_{\mu\nu\lambda\sigma} G_a^{\mu\nu} G_a^{\lambda\sigma}(x),$$

$$O_2(x) = -\frac{1}{2} \partial^\mu \sum_{i=1}^{n_f} \bar{q}_i(x) \gamma_\mu \gamma_5 q_i(x), \quad (4)$$

where $\Phi^H(x)$ and $\Phi^A(x)$ represent the scalar and pseudo-scalar fields respectively and n_f denotes the number of light flavours. Furthermore the gluon field strength is given by $G_a^{\mu\nu}$ and the quark field is denoted by q_i . The factors multiplying the operators are chosen in such a way that the vertices are normalised to the effective coupling constants G_H , G_A and \tilde{G}_A . The latter are determined by the top-quark triangular loop graph, including all QCD corrections, taken in the limit $m_t \rightarrow \infty$ which describes the decay process $B \rightarrow g + g$ with $B = H, A$ namely

$$\begin{aligned} G_B &= -2^{5/4} a_s(\mu_r^2) G_F^{1/2} \tau_B F_B(\tau_B) \\ &\times \mathcal{C}_B \left(a_s(\mu_r^2), \frac{\mu_r^2}{m_t^2} \right) \quad , \quad \tau = \frac{4m_t^2}{m^2}, \\ \frac{\tilde{G}_A}{G_A} &= - \left[a_s(\mu_r^2) C_F \left(\frac{3}{2} - 3 \ln \frac{\mu_r^2}{m_t^2} \right) + .. \right] \quad (5) \end{aligned}$$

where $a_s(\mu_r^2) = \alpha_s(\mu_r^2)/4\pi$ and μ_r denotes the renormalization scale. Further G_F represents the Fermi constant and the functions F_B are given in

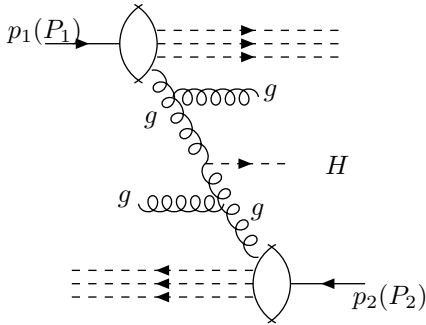


Figure 1. The reaction $p_1(P_1) + p_2(P_2) \rightarrow H + X'$.

the asymptotic limit by

$$\lim_{\tau \rightarrow \infty} F_H(\tau) = \frac{2}{3\tau}, \quad \lim_{\tau \rightarrow \infty} F_A(\tau) = \frac{1}{\tau} \cot \beta. \quad (6)$$

$\cot \beta$ denotes the mixing angle in the Two-Higgs-Doublet Model [3]. The coefficient functions C_B originate from the corrections to the top-quark triangular graph provided one takes the limit $m_t \rightarrow \infty$. They were computed up to order α_s^2 in [4], [5] for the H and in [6] for the A.

One tree diagram contributing to the reaction $p_1(P_1) + p_2(P_2) \rightarrow H + X'$ is shown in Fig. 1. On the Born level we have the partonic reaction

$$g(p_1) + g(p_2) \rightarrow B(p_5). \quad (7)$$

In NLO we have in addition to the one-loop virtual corrections to the above reaction the following two-to-two body processes

$$\begin{aligned} g + g &\rightarrow B + g, \quad g + q(\bar{q}) \rightarrow B + q(\bar{q}), \\ q + \bar{q} &\rightarrow B + g. \end{aligned} \quad (8)$$

Such diagrams contain the same basic building blocks as in the Drell-Yan production of dileptons (see the contribution of van Neerven to these proceedings). The LO and NLO contributions to the total cross section for H production were computed in [7]. The two-to-three body processes were computed for H and A production in [8] and

[9] respectively using helicity methods. The one-loop corrections to the two-to-two body reactions above were computed for the H in [10] and the A in [11]. These matrix elements were used to compute the transverse momentum and rapidity distributions of the H up to NLO in [12], [13] and the A in [11].

In NNLO we receive contributions from the two-loop virtual corrections to the Born process in Eq. (7) and the one-loop corrections to the reactions in Eq. (8). To these contributions one has to add the results obtained from several two-to-three body reactions containing gluons and quarks, e.g.

$$g(p_1) + g(p_2) \rightarrow g(p_3) + g(p_4) + B(p_5). \quad (9)$$

The effective Lagrangian method was also applied to obtain the NNLO total cross section for H production by the calculation of the two-loop corrections to the H-g-g vertex in [14], the soft-plus-virtual gluon corrections in [15], [16] and the computation of the two-to-three body processes in [17], [18], [19], [20]. These calculations were repeated for pseudo-scalar Higgs production in [21], [22] and [19], [20]. In the case of A production one also has to add the contributions due to interference terms coming from the operators O_1 and O_2 in Eq. (4), (see Fig. 1b and Fig. 2b of [21]).

Let us start with the NNLO virtual corrections. The most complicated diagram is the two-loop non-planar graph for $H(p_2-p_1) \rightarrow g(p_1) + g(-p_2)$ shown in Fig. 2. The momenta are incoming and k_1, k_2 label the two loop momenta.

The basic integral for this diagram has been known for a long time. It is

$$\begin{aligned} V_{123567} &= s^{-2} s^\varepsilon S_n^2 \left[-16 \varepsilon^{-4} + 24 \varepsilon^{-2} \zeta(2) \right. \\ &\quad \left. - \frac{166}{3} \varepsilon^{-1} \zeta(3) + \frac{177}{10} \zeta(2)^2 \right]. \end{aligned} \quad (10)$$

where $s = (p_1 - p_2)^2$ and S_n is the angular factor in $n = 4 + \varepsilon$ dimensions. In Drell-Yan production of lepton pairs the highest power of momenta in the numerator was three which required the result

$$(k_1 \cdot p_2)^3 V_{123567} = s s^\varepsilon S_n^2 \left[\frac{69}{8} + \varepsilon^{-4} - \frac{3}{2} \varepsilon^{-3} \right]$$

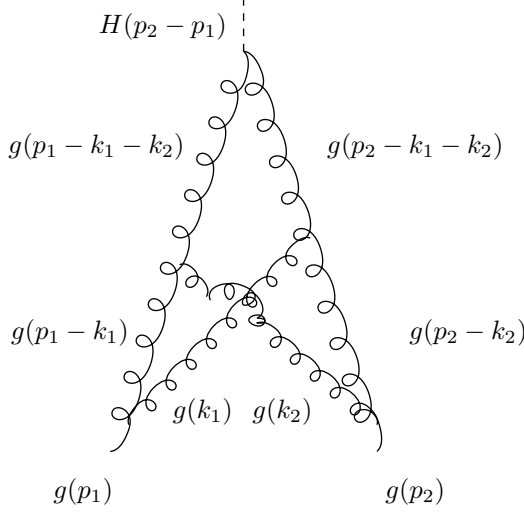


Figure 2. The two-loop non-planar crossed graph.

$$\begin{aligned}
& -\frac{3}{2}\varepsilon^{-2}\zeta(2) + 3\varepsilon^{-2} + \frac{15}{8}\varepsilon^{-1}\zeta(2) \\
& + \frac{83}{24}\varepsilon^{-1}\zeta(3) - \frac{21}{4}\varepsilon^{-1} - 3\zeta(2) \\
& - \frac{177}{160}\zeta(2)^2 - 5\zeta(3) \Big].
\end{aligned} \tag{11}$$

However in the Higgs case we need the integrals with up to four powers in the numerator such as

$$\begin{aligned}
(k_1 \cdot p_2)^4 V_{123567} = & s^2 s^\varepsilon S_n^2 \left[-\frac{56087}{10368} - \frac{1}{2}\varepsilon^{-4} \right. \\
& + \frac{11}{12}\varepsilon^{-3} + \frac{3}{4}\varepsilon^{-2}\zeta(2) - \frac{67}{36}\varepsilon^{-2} - \frac{55}{48}\varepsilon^{-1}\zeta(2) \\
& - \frac{83}{48}\varepsilon^{-1}\zeta(3) + \frac{2837}{864}\varepsilon^{-1} + \frac{67}{36}\zeta(2) \\
& \left. + \frac{177}{320}\zeta(2)^2 + \frac{55}{18}\zeta(3) \right].
\end{aligned} \tag{12}$$

The virtual corrections were calculated in [14] with the program Mincer [23] and we have checked them by using the methods in [24]. In the pseudoscalar case everyone used the HVBM

prescription for the γ_5 -matrix and the Levi-Civita tensor in [25], [26], [27].

The evaluation of the two-to-three body phase space integrals is possible in suitable frames. Since we integrate over the total phase space the integrals are Lorentz invariant and therefore frame independent. The matrix elements of the partonic reactions can be partial fractioned in such a way that maximally two factors $P_{ij} = (p_i + p_j)^2$ depend on the polar angle θ and the azimuthal angle ϕ . Furthermore only one factor depends on θ whereas the other one depends both on θ and ϕ . Therefore the following combinations show up in the matrix elements

$$P_{ij}^k P_{mn}^l, \quad P_{ij}^k P_{m5}^l, \quad P_{i5}^k P_{m5}^l,$$

$$4 \geq k \geq -2, \quad 4 \geq l \geq -2,$$

$$p_i^2 = p_j^2 = p_m^2 = p_n^2 = 0, \quad p_5^2 = m^2. \tag{13}$$

For the first combination it is easy to perform the angular integrations exactly in the CM frame of the incoming partons since all momenta represent massless particles. This requires the result in [24].

$$\begin{aligned}
& \int_0^\pi d\theta \int_0^\pi d\phi \sin^{n-3}\theta \sin^{n-4}\phi \mathcal{C}_{kl}(\theta, \phi, \chi) = \\
& 2^{1-k-l} \pi \frac{\Gamma(\frac{1}{2}n-1-k)\Gamma(\frac{1}{2}n-1-l)\Gamma(n-3)}{\Gamma(n-2-k-l)\Gamma^2(\frac{1}{2}n-1)} \\
& \times F_{1,2}\left(k, l, \frac{1}{2}n-1; \cos^2(\chi/2)\right),
\end{aligned} \tag{14}$$

where the function $\mathcal{C}_{ij}(\theta, \phi, \chi) = (1 - \cos\theta)^{-k} (1 - \cos\theta \cos\chi - \sin\theta \cos\phi \sin\chi)^{-l}$. Here $\cos\chi$ is related to kinematical variables such as x ($= m^2/s$, $\sqrt(s)$ =CM energy) and another two integration variables z and y , and $F_{1,2}(a, b, c; t)$ is the hypergeometric function.

The angular integral of the second combination is more difficult to compute because one particle is massive and the result is an one dimensional integral over a hypergeometric function which however can be expanded around ε . Examples of these types of integrals can be found in Appendix C of [28]. The last combination is very difficult to compute in n dimensions because both factors contain the massive particle indicated by p_5 . This

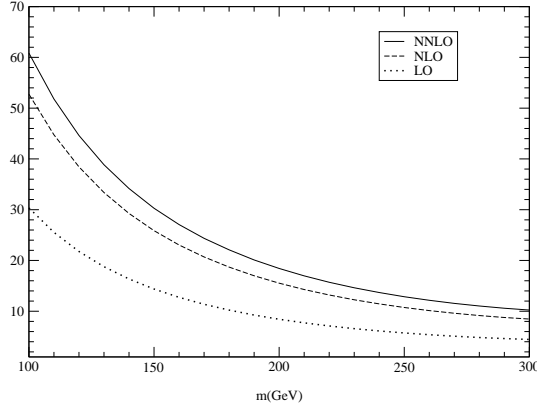


Figure 3. The total cross section σ_{tot} with all channels included plotted as a function of the Higgs mass at $\sqrt{S} = 14$ TeV with $\mu = m$

combination can be avoided if one chooses one of the following three frames, namely (1) the CM frame of the incoming partons, (2) the CM frame of the two outgoing partons indicated by the momenta p_3 and p_4 , and (3) the CM frame of one of the outgoing partons and the H indicated by the momenta p_4 and p_5 respectively

In (3) we performed one angular integration (say ϕ) exactly and performed the remaining θ integration after expanding the integrands in powers of $\varepsilon = n - 4$. In all these frames, using various Kummer's relations, the hypergeometric functions are simplified to the form $F_{1,2}(\pm\varepsilon/2, \pm\varepsilon/2, 1 \pm \varepsilon/2; f(x, y, z))$ which is the most suitable for integrations over z and y . The higher powers of $1/(1-z)^{\alpha+\beta\varepsilon}$ or $1/z^{\alpha+\beta\varepsilon}$, where $\alpha > 1$, were then reduced by successive integration by parts with exact hypergeometric functions until we arrived at terms in $1/(1-z)^{1+\beta\varepsilon}$ or $1/z^{1+\beta\varepsilon}$ multiplied by regular functions. This required the following identity

$$\begin{aligned} \frac{d}{dz} F_{1,2}(\varepsilon/2, \varepsilon/2, 1 + \varepsilon/2; f(z)) = \\ \frac{\varepsilon}{2f(z)} \frac{df(z)}{dz} \left((1 - f(z))^{-\frac{\varepsilon}{2}} \right. \\ \left. - F_{1,2}(\varepsilon/2, \varepsilon/2, 1 + \varepsilon/2; f(z)) \right). \end{aligned} \quad (15)$$

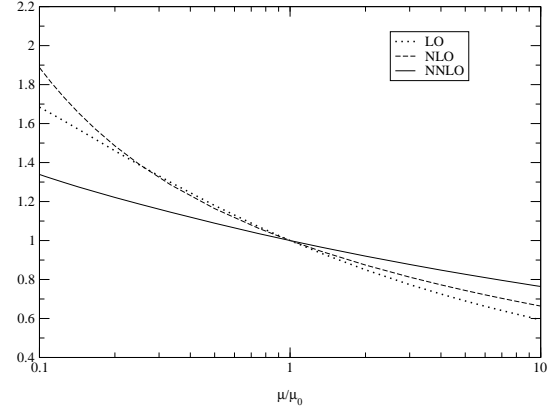


Figure 4. The quantity $N(\mu/\mu_0)$ plotted in the range $0.1 < \mu/\mu_0 < 10$ with $\mu_0 = m$ and $m = 100$ GeV/c².

The remaining integrals like $\int_0^1 dz z^{-1-\beta\varepsilon} f(z)$ and/or $\int_0^1 dz (1-z)^{-1-\beta\varepsilon} f(z)$ were simplified as follows:

$$\begin{aligned} \int_0^1 dz z^{-1-\beta\varepsilon} f(z) = \\ \int_0^\delta dz z^{-1-\beta\varepsilon} f(z) + \int_\delta^1 dz z^{-1-\beta\varepsilon} f(z), \end{aligned} \quad (16)$$

where $\delta \ll 1$. The first term can be evaluated to be $f(0)([-\beta\varepsilon]^{-1} + \ln \delta + [-\beta\varepsilon/2] \ln^2 \delta + \dots)$. After expanding $z^{-\beta\varepsilon}$ in powers of ε in the second term the z integration can be performed exactly order-by-order in ε with non-zero δ . At the end the δ dependence cancels in each order in ε . Since the z integration over the hypergeometric functions is nontrivial due to their complicated arguments, we expanded them in powers of ε prior to the z integration, using

$$\begin{aligned} F_{1,2}(\varepsilon/2, \varepsilon/2, 1 + \frac{\varepsilon}{2}; f(z)) = 1 \\ + \frac{\varepsilon^2}{4} \text{Li}_2(f(z)) + \frac{\varepsilon^3}{8} \left(\text{S}_{1,2}(f(z)) - \text{Li}_3(f(z)) \right) \\ + \frac{\varepsilon^4}{16} \left(\text{S}_{1,3}(f(z)) - \text{S}_{2,2}(f(z)) + \text{Li}_4(f(z)) \right) \\ \dots, \end{aligned} \quad (17)$$

where $S_{n,p}(z)$ is the Nielsen function, with $n, p \geq 1$ and $Li_n(z) = S_{n-1,1}(z)$ (see [29]).

We have repeated the same procedure to perform the remaining y integration. The integrals were programmed using FORM [30] by extending a program originally used to compute the NNLO coefficient functions of the Drell-Yan process in [31], [32]. After performing all these integrals, we removed all the ultraviolet divergences by coupling constant and operator renormalisation. The remaining collinear divergences are removed by mass factorisation. Then we are left with finite partonic cross sections which are folded with parton distribution functions to the compute hadronic cross section for inclusive H and A production.

Our method differs from the one presented in [17], [21] and the approach followed in [18], [22]. The authors in the latter references compute the total cross section using the Cutkosky [33] technique where one- and two-loop Feynman integrals are cut in certain ways. These Feynman integrals can be computed using various techniques (for more details see the references in [18]). The authors in [17] chose the more conventional method which was already used to compute the coefficient functions for the Drell-Yan process. However instead of an exact computation of the $2 \rightarrow 2$ and $2 \rightarrow 3$ body phase space integrals they expanded them around $x = m^2/s = 1$. Since the coefficient functions were known from the Drell-Yan reaction to be expressible in a finite number of polylogarithms like $Li_n(x)$, $S_{n,p}(x)$ and logarithms of the types $\ln^i x \ln^j(1-x)$, which are all multiplied by polynomials in x , one could expand these functions in the limit $x \rightarrow 1$ and match them with the expressions coming from the phase space integrals. In this way the coefficients in the expansion were determined.

In Fig. 3 we show the total cross section for H production in p-p collisions at the LHC. For the computation of the effective coupling constant G_B in Eq. (3) we choose the top quark mass $m_t = 173.4 \text{ GeV}/c^2$ and the Fermi constant $G_F = 1.16639 \times 10^{-5} \text{ GeV}^{-2} = 4541.68 \text{ pb}$. We used the parton densities in [34]. The cross sections for the A are about $9/4 \cot^2 \beta$ times those for the H. Next we study their variation with re-

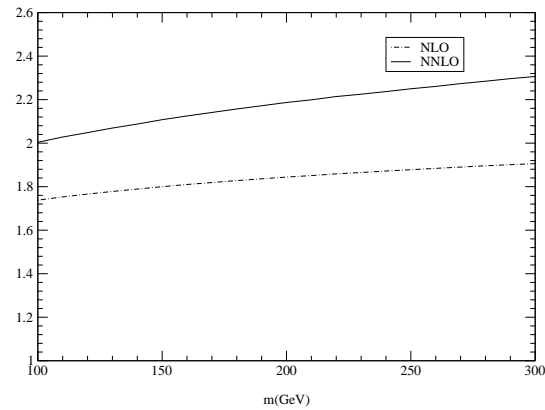


Figure 5. The K -factors in NLO and NNLO at $\sqrt{S} = 14 \text{ TeV}$ as a function of the Higgs mass using the MRST parton density sets; K^{NNLO} solid line, K^{NLO} dot-dashed line.

spect to the scale μ by computing the ratio

$$N\left(\frac{\mu}{\mu_0}\right) = \frac{\sigma_{\text{tot}}(\mu)}{\sigma_{\text{tot}}(\mu_0)}, \quad (18)$$

where $\mu_0 = m$ and μ is varied in the range $0.1 < \mu/\mu_0 < 10$. In Fig. 4 a plot of N is shown for $m = 100 \text{ GeV}/c^2$. Here one observes a clear improvement while going from LO to NNLO. In particular the curve for NNLO is flatter than that for NLO. Another way to estimate the reliability of this result is to study the rate of convergence of the perturbation series, which is represented by the K -factor. We choose the following definitions

$$K^{\text{NLO}} = \frac{\sigma_{\text{tot}}^{\text{NLO}}}{\sigma_{\text{tot}}^{\text{LO}}} \quad , \quad K^{\text{NNLO}} = \frac{\sigma_{\text{tot}}^{\text{NNLO}}}{\sigma_{\text{tot}}^{\text{LO}}}. \quad (19)$$

In Fig. 5 one observes that both K -factors vary slowly as m increases. Moreover there is considerable improvement in the rate of convergence if one goes from NLO to NNLO. At $m = 100 \text{ GeV}/c^2$ we have $K^{\text{NLO}} \sim 1.74$ whereas $K^{\text{NNLO}} \sim 2.00$. Still the corrections for Higgs boson production are larger than those obtained from Z -boson production at the LHC where one gets $K^{\text{NLO}} \sim 1.22$ and $K^{\text{NNLO}} \sim 1.16$ (see [32]).

REFERENCES

1. Tevatron Electroweak Working Group, [D0 Collaboration], hep-ex/0404010.
2. R. Barate et al, [ALEPH Collaboration], Phys. Lett. B 565 (2003) 61, hep-ex/0306033.
3. J.F. Gunion, H.E. Haber, G.L. Kane, S. Dawson, "The Higgs Hunter's Guide", Addison-Wesley, Reading 1990.
4. M. Krämer, E. Laenen, M. Spira, Nucl. Phys. B511 (1998) 523, hep-ph/9611272.
5. K.G. Chetyrkin, B.A. Kniehl, M. Steinhauser, Phys. Rev. Lett. 79 (1997) 353, hep-ph/9705240.
6. K.G. Chetyrkin, B.A. Kniehl, M. Steinhauser, W.A. Bardeen, Nucl. Phys. B535 (1998) 3, hep-ph/9807241.
7. S. Dawson, Nucl. Phys. B359 (1991) 283; A. Djouadi, M. Spira, P. Zerwas, Phys. Lett. B264 (1991) 440.
8. R.P. Kauffman, S.V. Desai, D. Risal, Phys. Rev. D55 (1997) 4005; Erratum-ibid, D58 (1998) 119901, hep-ph/9610541.
9. R.P. Kauffman, S.V. Desai, Phys. D59 (1999) 05704, hep-ph/9808286.
10. C.R. Schmidt, Phys. Lett. B413 (1997) 391, hep-ph/9707448.
11. B. Field, J. Smith, M.E. Tejeda-Yeomans, W.L. van Neerven, Phys. Lett. B551 (2002) 137, hep-ph/0210369.
12. D. de Florian, M. Grazzini, Z. Kunszt, Phys. Rev. Lett. 82 (1999) 5209, hep-ph/9902483.
13. V. Ravindran, J. Smith, W.L. van Neerven, Nucl. Phys. B634 (2002) 247, hep-ph/0201114.
14. R.V. Harlander, Phys. Lett. B492 (2000) 74, hep-ph/0007289.
15. S. Catani, D. de Florian, M. Grazzini, JHEP 0105 (2001) 025, hep-ph/0102227.
16. R.V. Harlander, W.B. Kilgore, Phys. Rev. D64 (2001) 013015, hep-ph/0102241.
17. R.V. Harlander, W.B. Kilgore, Phys. Rev. Lett. 88 (2002) 201801, hep-ph/0201206.
18. C. Anastasiou, K. Melnikov, Nucl. Phys. B646 (2002) 220, hep-ph/0207004.
19. V. Ravindran, J. Smith, W.L. van Neerven, Nucl. Phys. B665 (2003) 325. hep-ph/0302135.
20. V. Ravindran, J. Smith, W.L. van Neerven, Pramana 62 (2004) 683. hep-ph/0304005.
21. R.V. Harlander, W.B. Kilgore, JHEP 0210 (2002) 017, hep-ph/0208096.
22. C. Anastasiou, K. Melnikov, Phys. Rev. D67 (2003) 037501, hep-ph/0208115.
23. S.G. Gorishnii et al, Comput. Phys. Commun. 55 (1989) 381; S.A. Larin, F.V. Tkachov and J.A.M. Vermaseren, Rep. No. NIKHEF-H/91-18 (Amsterdam, 1991); available from <http://www.nikhef.nl/~form>.
24. W. L. van Neerven, Nucl. Phys. B268 (1986) 453.
25. G. 't Hooft, M. Veltman, Nucl. Phys. B44 (1972) 189.
26. P. Breitenlohner, B. Maison, Commun. Math. 53 (1977) 11, 39, 55.
27. D. Akyeampong, R. Delbourgo, Nuov. Cim. 17A (1973) 578, 18A (1973) 94, 19A (1974) 219.
28. W. Beenakker, H. Kuijf, W.L. van Neerven, J. Smith, Phys. Rev. D40 (1989) 54.
29. L. Lewin, "Polylogarithms and Associated Functions", North Holland, Amsterdam, 1983.
30. J.A.M. Vermaseren, Nucl. Phys. Proc. Suppl. 116 (2003) 343, hep-ph/0211297; version 3.0 available from <http://www.nikhef.nl/~form>.
31. T. Matsuura, S.C. van der Marck, W.L. van Neerven, Phys. Lett. B211 (1988) 171; ibid Nucl. Phys. B319 (1989) 570.
32. R. Hamberg, W.L. van Neerven, T. Matsuura, Nucl. Phys. B359 (1991) 343; Erratum-ibid Nucl. Phys. B644 (2002) 403.
33. R.E. Cutkosky, J. Math. Phys. 1 (1960) 429.
34. A.D. Martin, R.G. Roberts, W.J. Stirling, R.S. Thorne, Phys. Lett. B531 (2002) 216, hep-ph/0201127; Eur. Phys. J. C23 (2002) 73, hep-ph/0110215.